


## Peribiliary liver metastases MR findings

Vincenza Granata<sup>1</sup> · Roberta Fusco<sup>1</sup>  · Orlando Catalano<sup>1</sup> · Antonio Avallone<sup>2</sup> · Maddalena Leongito<sup>3</sup> · Francesco Izzo<sup>3</sup> · Antonella Petrillo<sup>1</sup>

Received: 10 May 2017 / Accepted: 24 May 2017 / Published online: 1 June 2017  
© Springer Science+Business Media New York 2017

**Abstract** We described magnetic resonance (MR) features of peribiliary metastasis and of periductal infiltrative cholangiocarcinoma. We assessed 35 patients, with peribiliary lesions, using MR 4-point confidence scale. T1-weighted (T1-W), T2-weighted (T2-W) and diffusion-weighted images (DWI) signal intensity, enhancement pattern during arterial, portal, equilibrium and hepatobiliary phase were assessed. We identified 24 patients with periductal-infiltrating cholangiocellular carcinoma. The lesions in 34 patients appeared as a single tissue, while in a single patient, the lesions appeared as multiple individual

lesions. According to the confidence scale, the median value was 4 for T2-W, 4 for DWI, 3.6 for T1-W in phase, 3.6 for T1-W out phase, 3 for MRI arterial phase, 3.2 for MRI portal phase, 3.2 for MRI equilibrium phase and 3.6 for MRI hepatobiliary phase. According to Bismuth classification, all lesions were type IV. In total, 19 (54.3%) lesions were periductal, 15 (42.9%) lesions were intraperiductal, and 1 (2.8%) lesion was periductal intrahepatic. All lesions showed hypointense signal in T1-W and in ADC maps and hyperintense signal in T2-W and DWI. All lesions showed a progressive contrast enhancement. There was no significant difference in signal intensity and contrast enhancement among all metastases and among all metastases with respect to CCCs, for all imaging acquisitions ( $p$  value  $>0.05$ ). MRI is the method of choice for biliary tract tumors thanks to the possibility to obtain morphological and functional evaluations. T2-W and DW sequences have highest diagnostic performance. MRI does not allow a correct differential diagnosis among different histological types of metastasis and between metastases and CCC.

---

✉ Roberta Fusco  
r.fusco@istitutotumori.na.it

Vincenza Granata  
v.granata@istitutotumori.na.it

Orlando Catalano  
o.catalano@istitutotumori.na.it

Antonio Avallone  
a.avallone@istitutotumori.na.it

Maddalena Leongito  
maddalena.leongito@virgilio.it

Francesco Izzo  
f.izzo@istitutotumori.na.it

Antonella Petrillo  
a.petrillo@istitutotumori.na.it

**Keywords** Liver metastasis · Peribiliary metastasis · Biliary tree · Magnetic resonance imaging

### Background

Peribiliary metastases are the most common solid malignancy of the bile ducts beyond cholangiocellular carcinoma (CCC) [1]. Although they are considered rare, it is likely that the true incidence is underestimated [1]. Cancers most frequently metastasizing to the biliary tract are those of the gastrointestinal tract, such as colorectal, gastric and pancreatic carcinoma. Also breast, lung and renal cancer, so as

<sup>1</sup> Radiology Division, Istituto Nazionale Tumori - IRCCS - Fondazione G. Pascale, Via Mariano Semmola, 80131 Naples, Italy

<sup>2</sup> Abdominal Oncology Division, Istituto Nazionale Tumori - IRCCS - Fondazione G. Pascale, Via Mariano Semmola, 80131 Naples, Italy

<sup>3</sup> Hepatobiliary Surgical Oncology Division, Istituto Nazionale Tumori - IRCCS - Fondazione G. Pascale, Via Mariano Semmola, 80131 Naples, Italy

melanoma and lymphoma, can metastasize to the biliary tract [1]. The site more often involved is the common hepatic duct, and the lesion appears as extra luminal, periductal tissue or as hepatoduodenal ligament lymph nodes metastasis [1, 2]. Proper detection and characterization of metastatic periductal lesions is crucial for patient management. Imaging studies does not allow a differential diagnosis with CCC, and sometimes from non-tumor lesions, due to an overlapping of radiological features [3]. Consequently, diagnosis was based on histological findings and on the patient medical history [3]. Multidetector computed tomography (MDCT) and magnetic resonance imaging (MRI) are the most common techniques employed to evaluate the liver and biliary tree [4]. MRI provides an assessment of the signal characteristics, vascularity and pathophysiology of different tumors due to its superior soft tissue contrast [5–9]. Additionally, various liver-specific contrast media (cm) have been developed to improve the lesions detection and characterization. Gadobenate dimeglumine (Gd-BOPTA) and gadolinium ethoxybenzyl diethylenetriamine pentaacetic acid (Gd-EOB-DTPA) can be injected as an intravenous bolus, providing data about lesion vascularity in the different phases of contrast circulation, while functional data can be obtained in the delayed, hepatobiliary phase [10]. In view of that, MRI is the preferred imaging modality for patients with suspected biliary tumors [1–4]; the purpose of this study is to identify the imaging MR features to detect and characterize a peribiliary metastasis.

## Materials and methods

### Patient population

Local Ethical Committee approval (“Comitato Etico IRRCS Pascale” of the National Cancer Institute of Naples) was obtained for this retrospective study. Informed consent was obtained from all individual participants included in the study. Through a computerized search of medical records, 35 oncological patients with an increase of bilirubin (between 4 and 16 mg/dL; mean value 8 mg/dL) and carbohydrate antigen (CA) 19.9 (between 60 and 148 U/mL; mean value 109 U/mL) with proven histological peribiliary metastases were identified who underwent gadolinium ethoxybenzyl diethylenetriamine pentaacetic acid (Gd-EOB-DTPA)-enhanced MRI from May 2012 to December 2016. As a control study group, we identified 24 consecutive patients with periductal-infiltrating cholangiocellular carcinoma (PI-CCC). All the data were collected and managed according to the privacy regulation in our country. In Table 1, we report the patient demographics data.

### MR imaging protocol

MR imaging was performed by a 1.5-T scanner (Magnetom Symphony, with Total Imaging Matrix Package, Siemens, Erlangen, Germany) with an 8-element body coil and a phased array coil. The MR examination consisted of images taken before IV injection of contrast medium and dynamic sequences obtained after injection of a liver-specific contrast medium Gd-EOB-DTPA (Primovist, Bayer Schering Pharma, Berlin, Germany). MR protocol is summarized in Table 2. Diffusion-weighted imaging (DWI) was obtained with planar echo-pulse sequence (*b* values 0, 50, 100, 200, 400, 600 and 800 s/mm<sup>2</sup>). All patients received 0.1 mL/kg of Primovist (5–10 mL, mean 8 mL) by means of a power injector (Spectris Solaris® EP MR, MEDRAD Inc., Indianola, USA), at a rate of 1 mL/s. VIBE T1-weighted fat-suppressed (SPAIR) sequences were acquired in four different phases, arterial phase (35-s delay), portal venous phase (90 s), equilibrium phase (120 s) and hepatobiliary excretion phase (20 min).

### Images analysis

Three radiologists with at least 10 years of experience in liver MR imaging recorded in consensus the data. We compared the imaging features among the study population and control study group. Presence, side and extent of the lesions on MRI study were categorized, using a 4-point confidence scale (score) [11]; 1, no lesion; 2, probably no lesion; 3, probably lesion; 4, definitely lesion. For each single lesion, the radiologists recorded the signal intensity (SI) of T1-W images, T2-W images, DW images and of the apparent diffusion coefficient (ADC) map. We analyzed the contrast enhancement during the arterial, portal, equilibrium and hepatobiliary phase of MR study. The tumor location was classified, according to Bismuth [12, 13] in: type I, limited to the common hepatic duct, below the level of the confluence of the right and left hepatic ducts; type II, involving the confluence of the right and left hepatic ducts; type IIIa involving the confluence of the right and left hepatic ducts and extending to the bifurcation of the right hepatic duct; type IIIb involving the confluence of the right and left hepatic ducts and extending to the bifurcation of the left hepatic duct; type IV extending to the bifurcations of both right and left hepatic ducts or multifocal involvement; and type V, stricture at the junction of common bile duct and cystic duct. Also, as intraductal, periductal, intraperiductal or periductal intrahepatic, in relation to the site of the lesion, with respect to the bile duct and liver parenchyma. The SI of the lesions in T1-W, T2-W, DWI and in ADC map was categorized as isointense, hypointense and hyperintense compared to surrounding liver parenchyma. We measured the ADC of each lesion. When

**Table 1** Patient demographics data

Description	Numbers (%)
Gender	Men 17 (48.6%) Women 18 (51.4%)
Age	58 (range 42–80)
Concomitant or previous history of	
Colorectal adenocarcinoma	12
Breast cancer	7
Pancreatic adenocarcinoma	7
Gastric adenocarcinoma	5
Endometrial cancer	1
Ovarian cancer	3
Concomitant and previous history of liver intraparenchymal metastases	8 (22.8%) and 19 (54.3%)
Clinical symptoms	
Abdominal pain	12 (34.3%)
Jaundice	28 (80.0%)
Pruritus	18 (51.4%)
Increase <i>n</i> tumor markers	35 (100.0%)
Systemic symptoms (weight loss or anemia)	5 (14.3%)

**Table 2** Pulse sequence parameters on MR studies

Sequence	Orientation	TR/TE/FA (ms/ms/°)	AT (min)	Image size	ST/gap (mm)	FS
TRUFISP T2-W	Coronal	4.30/2.15/80	0.46	512 × 512	4/0	Without
HASTE T2-W	Axial	1500/90/170	0.36	320 × 320	5/0	Without and with (SPAIR)
HASTE T2-W	Coronal	1500/92/170	0.38	320 × 320	5/0	Without
In–out phase T1-W	Axial	160/2.35/70	0.33	256 × 192	5/0	Without
DWI	Axial	7500/91/90	7	192 × 192	3/0	Without
VIBE T1-W	Axial	4.80/1.76/12	0.18	320 × 260	3/0	With (SPAIR)

*TR* repetition time, *TE* echo time, *FA* flip angle, *AT* acquisition time, *ST* slice thickness, *FS* fat suppression, *SPAIR* spectral adiabatic inversion recovery

the lesion was hyperintense on all *b* values we defined this restricted diffusion. The DW signal decay was analyzed using a linear fitting of the mono-exponential model, according to the equation  $ADC = \ln(S_0/S_b)/b$ , where  $S_b$  is the signal intensity with diffusion weighting *b* ( $b > 200 \text{ s/mm}^2$ ) and  $S_0$  is the non-diffusion-weighted signal intensity. This analysis was based on multiple circular regions of interest (ROIs) of 0.3–0.9  $\text{cm}^2$  of size using median value of single voxel signals for each *b* value. ROI for the lesion was manually drawn to include hyperintense voxels on image at *b* value of 800  $\text{s/mm}^2$ . Median diffusion parameter of ROI was used as representative value for each lesion. No motion correction algorithm was used, but ROIs were drawn taking care to exclude areas in which movement artifacts or blurring caused voxel misalignments. The data analysis was performed using in-house software written in MATLAB (The MathWorks, Inc., Natick, USA).

We also recorded whether the enhancement was homogeneous, heterogeneous or progressive. Other aspects evaluated included: the presence of biliary tree dilatation, the presence of perilesional changes in vascular perfusion during the arterial phase, the presence of perilesional changes in signal intensity during the hepatobiliary phase, the signal intensity of the biliary ducts during the hepatobiliary phase.

Also, we compared the MRI features of peribiliary metastases and of PI-CCC.

**Statistical analysis**

Fisher’s exact test was employed to analyze differences in the location, signal intensity and contrast enhancement among metastases of different histological type and between metastases and PI-CCC. Mann–Whitney test was employed to analyze the differences in ADC median values among metastases of different histotypes and between

metastases and PI-CCC. A  $p$  value  $<0.05$  was regarded as statistically significant. Statistical analysis was obtained by means of the Statistic Toolbox of MATLAB (The MathWorks, Inc., Natick, USA).

## Results

MR detected all lesions. The lesions in 34 patients appeared as a single tissue that extended along the biliary tree. In a single patient, with breast cancer, the lesions appeared as multiple individual lesions and each of them that extended along the bile branches of second order (Fig. 1). According to the confidence scale, the median value obtained, in accordance with all radiologists, was 4 for T2-W HASTE, 4 for DWI, 3.6 for T1-W in phase, 3.6 for T1-W out phase, 3 for MRI arterial phase, 3.2 for MRI portal phase, 3.2 for MRI equilibrium phase and 3.6 for MRI hepatobiliary phase.

According to Bismuth classification, all lesions were type IV, while, in relation to the site of the lesion, with respect to the bile duct and hepatic parenchyma, 19 (54.3%) lesions were periductal (Fig. 2), 15 (42.9%) lesions were intraperiductal, and 1 (2.8%) lesion was periductal intrahepatic (in a patient with endometrial cancer). There was no exclusively intraductal lesion. The median score obtained in the assessment of tumor extent was 4 for T2-W HASTE, 4 for DWI, 3.6 for T1-W in

phase, 3.6 for T1-W out phase, 3.4 for MRI arterial phase, 3 for MRI portal phase, 3 for MRI equilibrium phase and 3.6 for MRI hepatobiliary phase.

All lesions showed hypointense signal on T1-W in-out phase images (Fig. 3), in precontrast VIBE T1-W images and in ADC maps, hyperintense signal on T2-W imaging (Fig. 3) and DWI (Fig. 4). The diffusion was restricted from  $b_0$  to  $b_{800}$   $s/mm^2$ , and the median ADC value was of  $1.27 \times 10^{-3}$   $mm^2/s$  (range  $1.01$ – $1.68 \times 10^{-3}$   $mm^2/s$ ). All lesions showed a progressive contrast enhancement (Fig. 5). All lesions were isohypointense in hepatobiliary phase (Fig. 6). There was no significant difference in signal intensity and contrast enhancement among all metastases on all imaging acquisitions ( $p$  value  $>0.05$ ).

All CCCs (Fig. 7) showed a hypointense signal on T1-W flash in-out phase images, in precontrast VIBE T1-W images and in ADC maps, and a hyperintense signal on T2-W and in DW images. The diffusion was restricted from  $b_0$  to  $b_{800}$   $s/mm^2$ , and the mean ADC value was of  $1.32 \times 10^{-3}$   $mm^2/s$  (range  $1.18$ – $1.57 \times 10^{-3}$   $mm^2/s$ ) (Fig. 8). There was no statistically significant difference in median ADC ( $p$  value  $>0.05$ ). CCCs showed a progressive contrast enhancement.

We found no significant difference in signal and contrast enhancement among all metastases with respect to CCCs on all imaging acquisitions ( $p$  value  $>0.05$ ). The only difference identified was in the extent of disease, with metastases penetrating deeper along the ducts of the

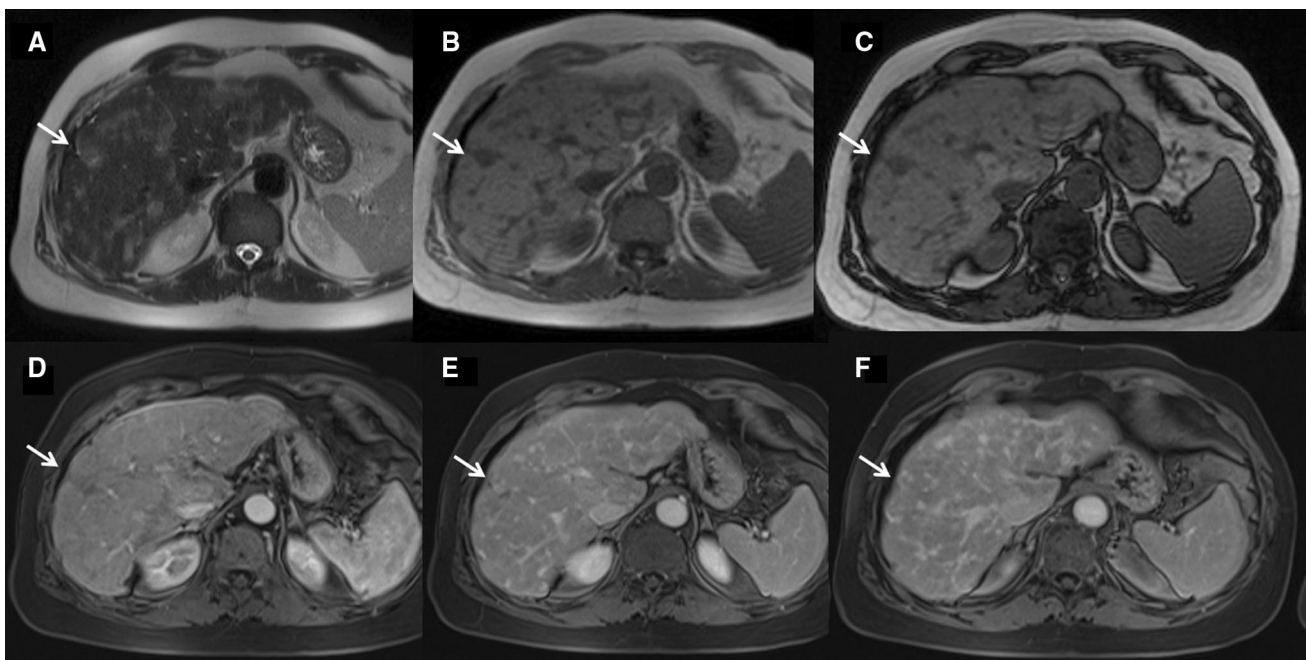


**Fig. 1** Sixty-five-year-old woman with breast cancer. The lesions appeared as multiple individual lesions and each of them that extended along the bile branches of second order. In **a** (T2-W HASTE axial plane), the lesion (*arrow*) appears hyperintense. In **b** (axial T1-

W in phase) and **c** (axial T1-W out phase), the lesion (*arrow*) shows hypointense signal. During arterial (**d**), portal (**e**) and equilibrium (**f**) phase of contrast study, the lesion has a progressive contrast enhancement

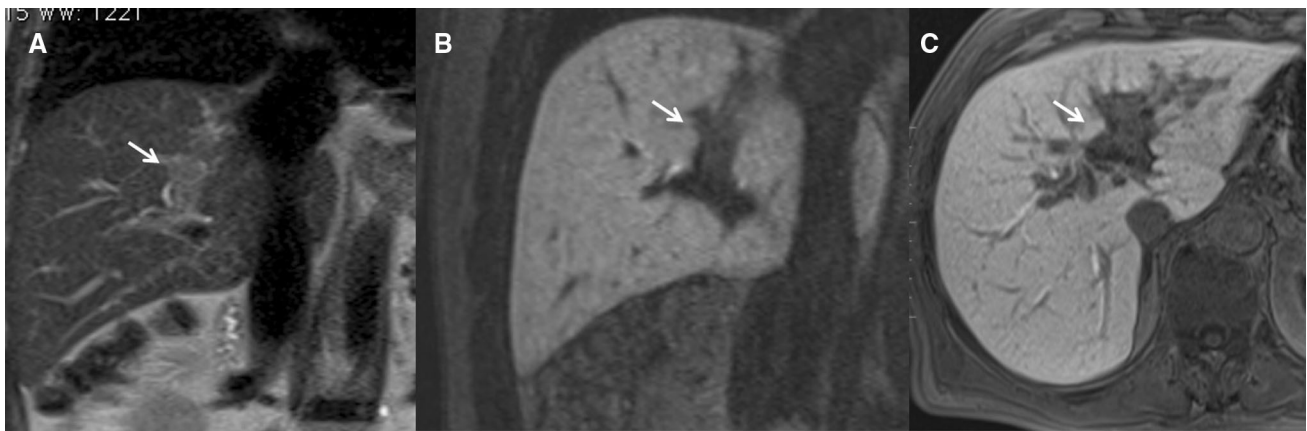


**Fig. 2** Forty-four-year-old man with rectal cancer. It is evident the presence (*arrow*) of peribiliary tissue as a hyperintense mass (in **a**; coronal T2-W HASTE) extending to the bifurcations of both right and

left hepatic ducts. In hepatobiliary phase (**b** coronal plane; **c** axial plane), the lesion appears as isohypointense tissue

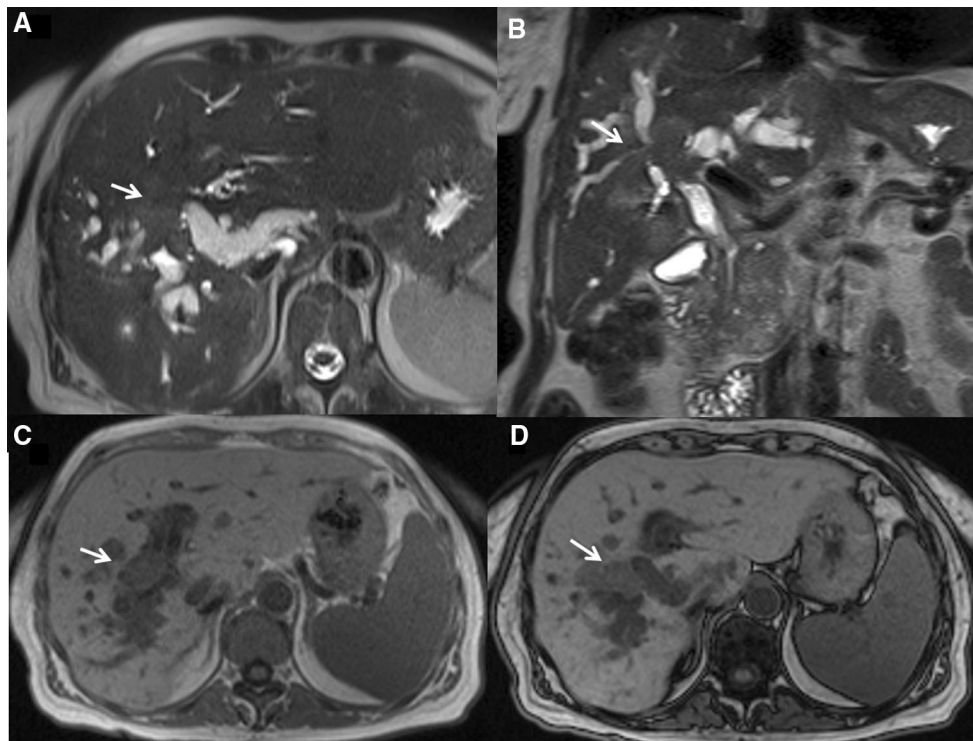


**Fig. 3** Sixty-three-year-old man with pancreatic cancer. Interruption of confluence of the right and left hepatic ducts with biliary tree dilatation. In **a** (axial T2-W HASTE) and **b** (coronal T2-W HASTE), it

is evident the presence of periductal hyperintense tissue (*arrow*) that appears hypointense (*arrow*) in **c** (axial T1-W in phase) and **d** (axial T1-W out phase)

second order and CCC showing a minor lesser longitudinal extension. However, this difference was not significant ( $p$  value  $>0.05$ ).

In all patients, we found biliary tree dilatation, with a degree of dilatation that correlate with the size of the lesion. When the tumor was of the periductal-intraductal type, the degree of dilatation was higher than that for

exclusively periductal and periductal-intrahepatic lesions. No change in perilesional vascular perfusion hepatic parenchyma and perilesional hepatic parenchyma during hepatobiliary phase was identified. In all patients, the biliary ducts adjacent to the metastasis did not eliminate the contrast medium in the hepatobiliary phase.

In Table 3, we summarized our results.

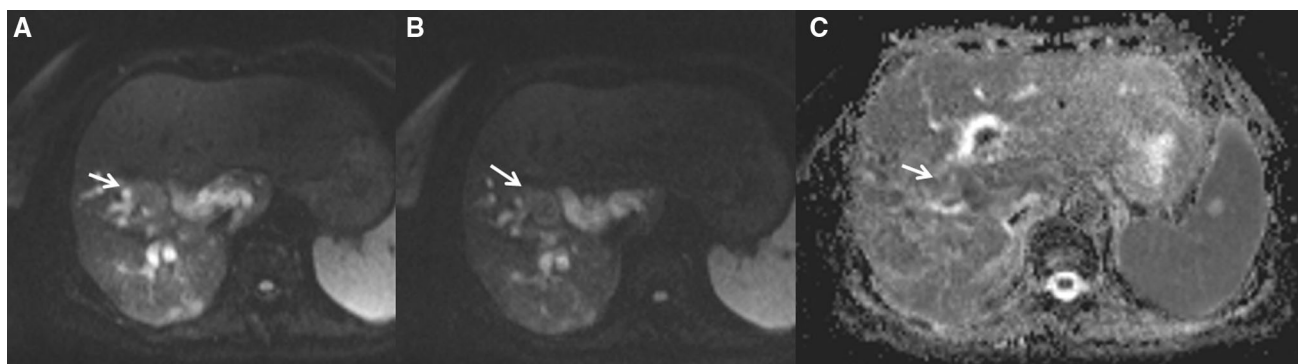


**Fig. 4** The same patient of Fig. 3. DWI sequences. In **a**  $b50 \text{ s/mm}^2$ , in **b**  $b800 \text{ s/mm}^2$ , in **c** ADC map. The tumor (arrow) shows restricted diffusion

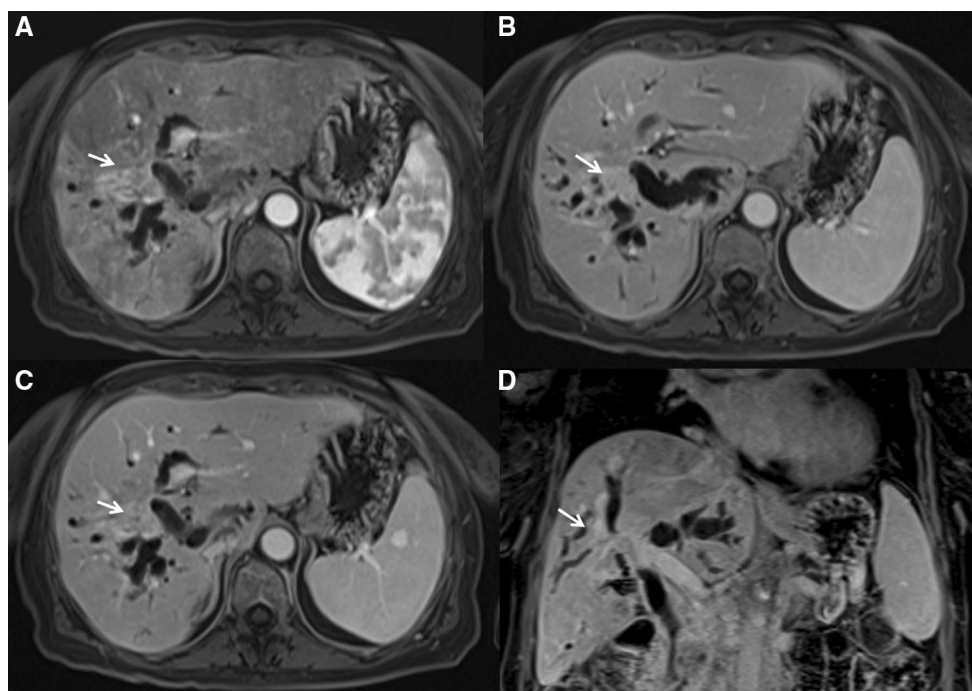


**Fig. 5** The same patient of Figs. 3 and 4. The lesion shows a progressive contrast enhancement from arterial phase (in **a** VIBE T1-W FS in axial plane) to portal (**b** VIBE T1-W FS in axial plane) and equilibrium phase (**c** VIBE T1-W FS in axial plane and coronal plane in **d**)

## Discussion

We evaluated 35 oncological patients with proven peribiliary metastases from different primitive neoplasm, and according to previous studies, in our series, the colorectal, gastric and pancreatic cancer was tumors that most often metastasize to biliary tree [1–5]. Twenty-four patients (68.6%) had concomitant and previous history of liver intraparenchymal metastases, while in 11 (31.4%) patients peribiliary site was the only hepatic location of metastatic disease. To the best of our knowledge, this is the first study that analyzes a large group of patients with peribiliary metastases, assessing not only the diagnostic performance of different sequences of MR but also analyzing

morphological and functional features to characterize the lesion. In our series MR detected all lesions, with the best performance obtained by T2-W sequences and DWI, thanks to high soft tissue contrast resolution. While the progressive contrast enhancement of lesions reduced the ratio signal/lesion on postcontrast sequences, the diagnostic accuracy of those was lower compared to T2-W sequences. MRI is the gold standard, in oncological examination, providing morphological and functional data. MR provides preoperative assessment of important prognostic outlines, which may guide patient treatment [6–9, 14–18]. The European Society of Gastrointestinal and Abdominal Radiology (ESGAR) Working Group suggested, using of MRI in the study of liver and biliary tree, not only with

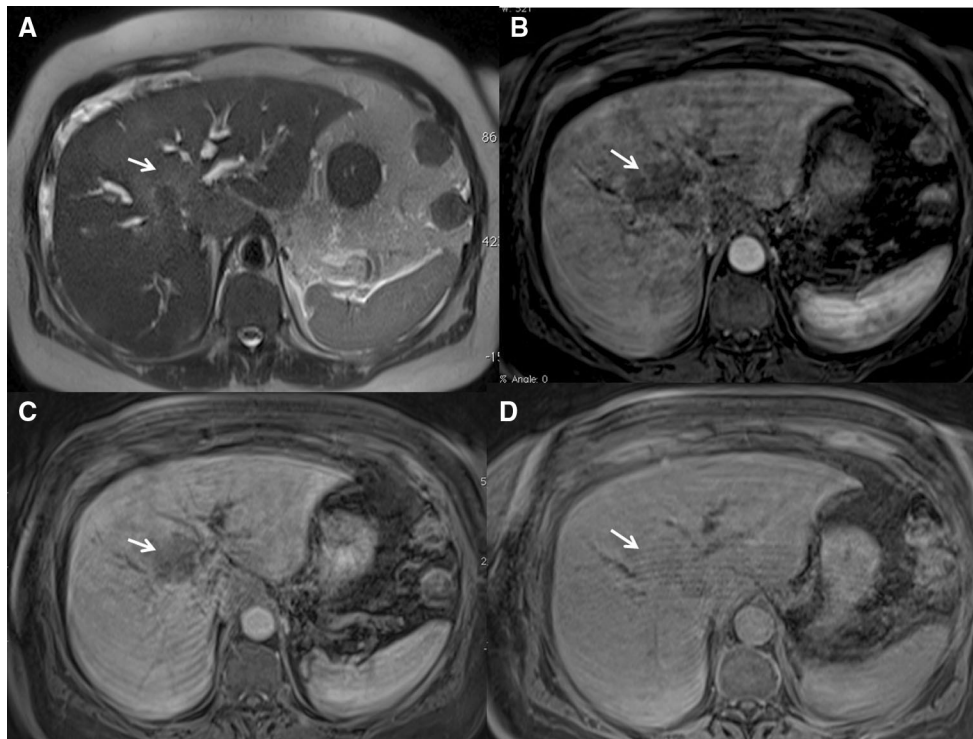


**Fig. 6** Fifty-six-year-old woman with breast cancer. The lesion (*arrow*) shows hyperintense signal in **a** (axial T2-W HASTE) extending to the bifurcations of both right and left hepatic ducts. After contrast medium, it is evident a progressive contrast

enhancement from arterial phase (in **b** VIBE T1-W FS in axial plane) to equilibrium phase (**c** VIBE T1-W FS in axial plane). In hepatobiliary phase (**d** axial plane), the lesion appears isohypointense

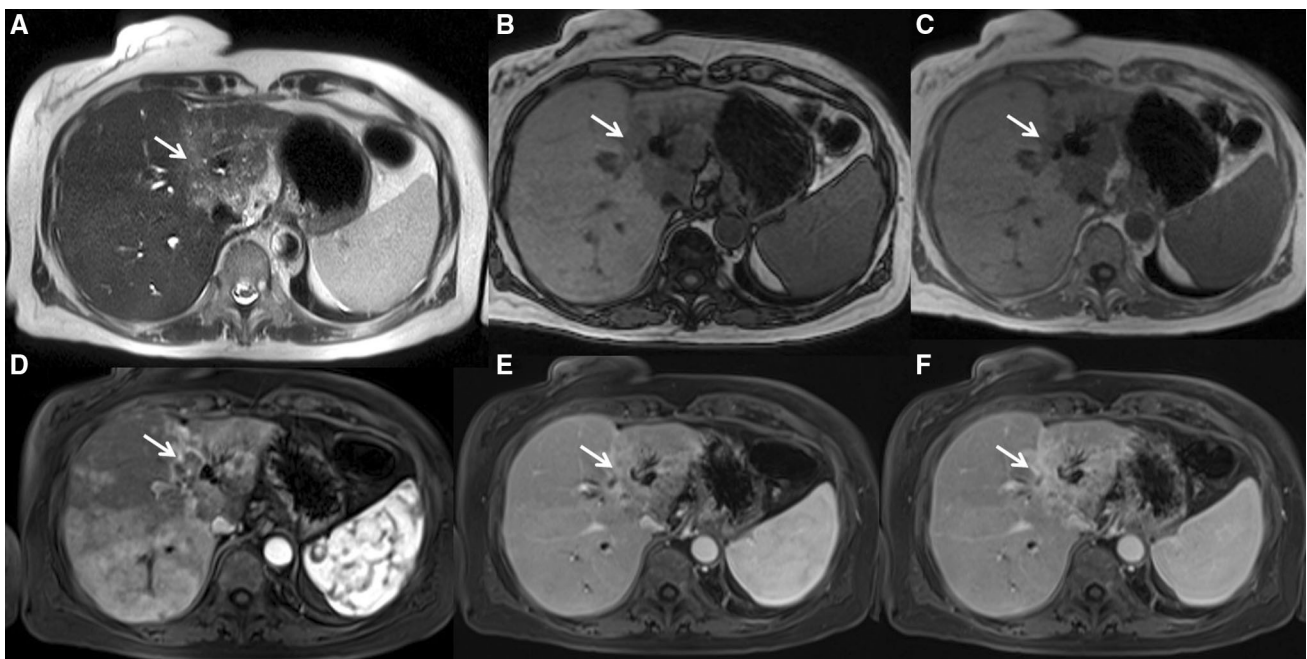


**Fig. 7** Fifty-seven-year-old man with CCC. In **a** (axial T2-W HASTE), the tumor (*arrow*) appears hyperintense. In **b** (axial T1-W out phase) and **c** (axial T1-W in phase), the lesion (*arrow*) shows

hypointense signal. During the arterial phase (**d**), portal (**e**) and equilibrium (**f**) phase, the lesion shows progressive contrast enhancement

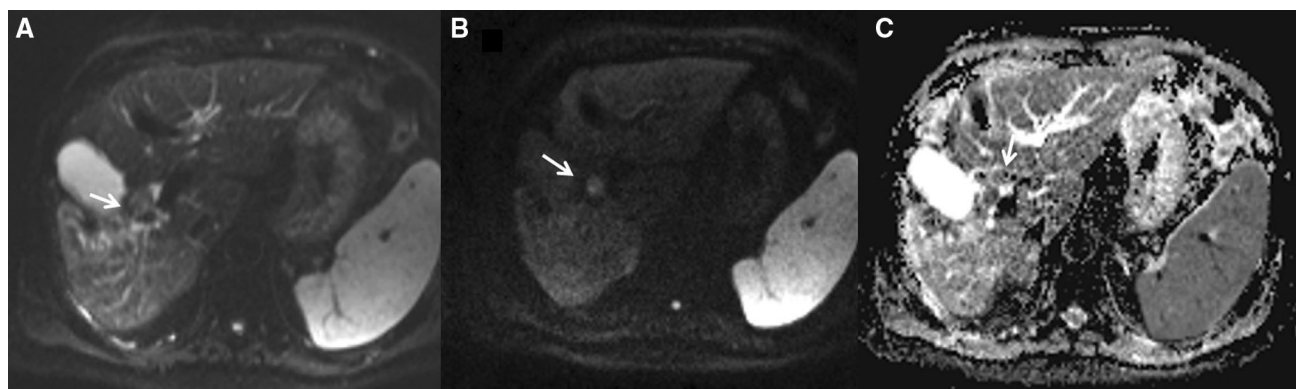


**Fig. 8** Sixty-seven-year-old man with CCC. In **a**  $b50 \text{ s/mm}^2$ , in **b**  $b800 \text{ s/mm}^2$  and in **c** ADC map. The tumor (*arrow*) shows restricted diffusion

**Table 3** Peribiliary metastases MR features

Description	Numbers (%)
Single lesion	34 (97.1%)
Multiple individual lesions	1 (2.9%)
Side	
IV	35 (100.0%)
Periductal	19 (54.3%)
Intraperiductal	15 (42.8%)
Periductal intrahepatic	1 (2.8%)
Sequence	Feature
T1-W in-out phase	Hypointense signal
Haste T2-W	Hyperintense signal
DWI	Restricted from $b0$ to $b800 \text{ s/mm}^2$ (SI: hyperintense)
ADC	Median value: $1.27 \times 10^{-3} \text{ mm}^2/\text{s}$ (range $1.01\text{--}1.68 \times 10^{-3} \text{ mm}^2/\text{s}$ ) (SI: hypointense)
Vibe pre cm	Hypointense signal
Vibe in arterial, portal and equilibrium phase	Progressive contrast enhancement
Vibe in hepatospecific phase	Hypointense signal

morphological sequences but also with DW imaging, perfusion acquisitions and cholangiopancreatographic acquisitions [19]. Our study protocol includes morphological (T1-W and T2-W) and functional (contrast study with hepatospecific contrast agent and DWI) sequences, to maximize the tumor detection rate and to evaluate the real lesion's extension. The accurate mapping of these lesions is necessary to choose the best surgical strategy and to identify patients unfit for surgery [4, 5, 20]. It is known that Gd-EOB-DTPA MRI is the technique to choose to evaluate liver metastases in presurgical setting [20]. Chung et al. [21] compared the diagnostic accuracy for liver metastases between Gd-EOB-DTPA MRI and DWI, showing that Gd-

EOB-DTPA MRI was more useful for the detection of metastases, while DWI was more accurate in their characterization. The combination of Gd-EOB-DTPA MRI and DWI had significantly higher accuracy and sensitivity for the preoperative detection of small colorectal liver metastases than DWI alone [21]. Also Donati et al. evaluated the association of Gd-EOB-DTPA MRI and DWI, demonstrating that the confidence, in final diagnosis, was significantly higher combining EOB-MRI and DWI data in comparison with DWI data alone. Adding DWI to Gd-EOB-DTPA MRI did not significantly increase diagnostic accuracy compared to Gd-EOB-DTPA MRI alone [22]. Conversely, when we analyzed the hepatospecific phase, compared to T2-W and DWI sequences, the diagnostic performance was lower (score of 3.6 compared to 4); this was because in our series the lesion was not intraparenchymal. In fact, in this case the lesion not appeared as a more hypointense tissue as an intraparenchymal lesion on hepatospecific phase [6]. Although EOB-Gd-DTPA not improved the detection rate of lesions, this cm provided functional data: The biliary ducts adjacent to the metastasis did not eliminate the contrast medium in the hepatobiliary phase.

The lesions showed a progressive contrast enhancement that reduced the ratio signal/lesion, so that the diagnostic performance of arterial, portal and equilibrium phase was lower than T2-W sequences and T1-W without cm and in hepatospecific phase. We found that all lesions showed this feature. Our data also showed that morphological T2-W sequences and DWI were indispensable in the study protocol to detect and staging peribiliary lesions. Our results were similar to those by Park et al. [23] that evaluated the incremental benefit of adding DW imaging to gadoteric acid-enhanced MR imaging and MR cholangiopancreatography in the preoperative evaluation of hilar CCC. In fact, DWI improved the assessment of tumor extent along the bile duct [23]. Differently from Choi [24] we found that the addition of DWI to morphological MRI was helpful in



establishing whether the secondary biliary confluence, bilaterally, was involved, while according to Choi [24], DWI did not improve in our series the diagnostic performance in the characterization of perihilar strictures. In fact, in our study DWI was not helpful in the differential diagnosis between the different metastatic histotypes and between metastases and CCC, because there was an overlapping between signal and ADC values among them. The MRI was not able to distinguish different histological types of peribiliary metastases and the different metastases from CCC. In fact, we found that there was no significant difference in signal and contrast enhancement among metastases and CCC in all morphological and functional sequences. The only difference we could identify was in the extent of disease, with metastases entering more deeply along the second-order ducts than CCC; however, this difference was not significant.

Our study has some limitations; first of all, it was a retrospective study, requiring further prospective assessment. Additionally, the reviewers evaluated the images in consensus, so we could not assess the interobserver reproducibility and at last, we did not have a control group of benign periductal diseases, to assess the differences between oncological and non-oncological patients.

## Conclusion

Although peribiliary metastases are uncommon, they can occur, especially in patients with gastroenteric cancer. So a proper detection and characterization is crucial for patient management. MRI, thanks to the possibility to obtain morphological and functional data, is the imaging technique of choice. T2-W and DW sequences have the highest diagnostic performance, while the typical lesion progressive contrast enhancement reduced the ratio signal/lesion, so that the diagnostic performance of contrast phase was lower than T2-W. EOB-Gd-DTPA did not improve the detection rate of lesions; however, this cm provides biliary functional data.

Finally, MRI not allows a correct differential diagnosis between the different histological metastases and between metastases and CCC, because of the overlapping features.

**Acknowledgements** The authors are grateful to Alessandra Trocino, librarian, at the National Cancer Institute of Naples, Italy. Moreover, for the collaboration, authors are grateful to Maria Bruno, Laura Galeani, Rita Guarino, Leandro Eto and Assunta Zazzaro.

**Author's contributions** VG, AP, FI conceived of the study and participated in its design, coordination and drafting of the manuscript. VG, RF participated in the studies collection and analyzed the data. VG, RF drafted the manuscript. VG, AP, FI, OC, AA, ML participated in the studies collection. All authors read and approved the final manuscript.

## Compliance with ethical standards

**Conflict of interest** The authors declare that they have no conflict of interest.

**Ethical approval** Local Ethical Committee approval (“Comitato Etico IRRCS Pascale” of the National Cancer Institute of Naples) was obtained for this retrospective study.

**Informed consent** Informed consent was obtained from all individual participants included in the study.

## References

1. Moon SG, Han JK, Kim TK, et al. Biliary obstruction in metastatic disease: thin-section helical CT findings. *Abdom Imaging*. 2003;28:45–52.
2. Popp JW, Schapiro RH, Warshaw AL. Extrahepatic biliary obstruction caused by metastatic breast carcinoma. *Ann Intern Med*. 1979;91:568–71.
3. Gwon DI, Ko GY, Sung KB, et al. Clinical outcomes after percutaneous biliary interventions in patients with malignant biliary obstruction caused by metastatic gastric cancer. *Acta Radiol*. 2012;53:422–9.
4. Corona-Villalobos CP, Pawlik TM, Kamel IR. Imaging of the patient with a biliary tract or primary liver tumor. *Surg Oncol Clin N Am*. 2014;23:189–206.
5. Mittal PK, Moreno CC, Kalb B, et al. Primary biliary tract malignancies: MRI spectrum and mimics with histopathological correlation. *Abdom Imaging*. 2015;40:1520–57.
6. Granata V, Catalano O, Fusco R, et al. The target sign in colorectal liver metastases: an atypical Gd-EOB-DTPA “uptake” on the hepatobiliary phase of MR imaging. *Abdom Imaging*. 2015;40:2364–71.
7. Granata V, Fusco R, Catalano O, et al. Intravoxel incoherent motion (IVIM) in diffusion-weighted imaging (DWI) for hepatocellular carcinoma: correlation with histologic grade. *Oncotarget*. 2016. doi:10.18632/oncotarget.12689.
8. Petrillo A, Fusco R, Petrillo M, et al. Standardized index of shape (DCE-MRI) and standardized uptake value (PET/CT): two quantitative approaches to discriminate chemo-radiotherapy locally advanced rectal cancer responders under a functional profile. *Oncotarget*. 2016. doi:10.18632/oncotarget.14106.
9. Granata V, Fusco R, Reginelli A, et al. Radiological assessment of anal cancer: an overview and update. *Infect Agent Cancer*. 2016;12(11):52.
10. Granata V, Cascella M, Fusco R, et al. Immediate adverse reactions to gadolinium-based MR contrast media: a retrospective analysis on 10,608 examinations. *Biomed Res Int*. 2016;2016:3918292.
11. Granata V, Petrillo M, Fusco R, et al. Surveillance of HCC patients after liver RFA: role of MRI with hepatospecific contrast versus three-phase CT scan-experience of high volume oncologic institute. *Gastroenterol Res Pract*. 2013;2013:469097.
12. Bismuth H, Corlette MB. Intrahepatic cholangioenteric anastomosis in carcinoma of the hilus of the liver. *Surg Gynecol Obstet*. 1975;140:170–8.
13. Chung YE, Kim MJ, Park YN, et al. Staging of extrahepatic cholangiocarcinoma. *Eur Radiol*. 2008;18(10):2182–95.
14. Zech CJ, Schoenberg SO, Reiser M, et al. Cross-sectional imaging of biliary tumors: current clinical status and future developments. *Eur Radiol*. 2004;14:1174–87.
15. Granata V, Fusco R, Catalano O, et al. Early assessment of colorectal cancer patients with liver metastases treated with

- antiangiogenic drugs: the role of intravoxel incoherent motion in diffusion-weighted imaging. *PLoS ONE*. 2015;10:e0142876.
16. Fusco R, Sansone M, Petrillo M, et al. Multiparametric MRI for prostate cancer detection: preliminary results on quantitative analysis of dynamic contrast enhanced imaging, diffusion-weighted imaging and spectroscopy imaging. *Magn Reson Imaging*. 2016;34(7):839–45.
  17. Fusco R, Sansone M, Filice S, et al. Integration of DCE-MRI and DW-MRI quantitative parameters for breast lesion classification. *Biomed Res Int*. 2015;2015:237863.
  18. Granata V, Fusco R, Catalano O, et al. Percutaneous ablation therapy of hepatocellular carcinoma with irreversible electroporation: MRI findings. *AJR Am J Roentgenol*. 2015;204(5):1000–7.
  19. Neri E, Bali MA, Ba-Ssalamah A, et al. ESGAR consensus statement on liver MR imaging and clinical use of liver-specific contrast agents. *Eur Radiol*. 2016;26:921–31.
  20. Van Cutsem E, Cervantes A, Adam R, et al. ESMO consensus guidelines for the management of patients with metastatic colorectal cancer. *Ann Oncol*. 2016;27:1386–422.
  21. Chung WS, Kim MJ, Chung YE, et al. Comparison of gadoxetic acid-enhanced dynamic imaging and diffusion-weighted imaging for the preoperative evaluation of colorectal liver metastases. *J Magn Reson Imaging*. 2011;34(2):345–53.
  22. Donati OF, Fischer MA, Chuck N, et al. Accuracy and confidence of Gd-EOB-DTPA enhanced MRI and diffusion-weighted imaging alone and in combination for the diagnosis of liver metastases. *Eur J Radiol*. 2013;82:822–8.
  23. Park MJ, Kim YK, Lim S, et al. Hilar cholangiocarcinoma: value of adding DW imaging to gadoxetic acid-enhanced MR imaging with MR cholangiopancreatography for preoperative evaluation. *Radiology*. 2014;270:768–76.
  24. Choi KS, Lee JM, Joo I, Han JK, et al. Evaluation of perihilar biliary strictures: does DWI provide additional value to conventional MRI? *AJR Am J Roentgenol*. 2015;205:789–96.